Relationship Between Insulin Sensitivity and Sphingomyelin Signaling Pathway in Human Skeletal Muscle

Marek Straczkowski,[1] Irina Kowalska,[1] Agnieszka Nikolajuk,[1] Stella Dzienis-Straczkowska,[1] Ida Kinalska,[1] Marcin Baranowski,[2] Malgorzata Zendzian-Piotrowska,[2] Zofia Brzezinska,[3] and Jan Gorski[2]

In vitro studies revealed that insulin resistance might be associated with the intracellular formation of ceramide, the second messenger in the sphingomyelin signaling pathway. The aim of the present study was to examine the content and composition of fatty acids in ceramide and sphingomyelin in human muscle and to evaluate their relationships with insulin sensitivity. The study was conducted on 27 male subjects with normal glucose tolerance. Euglycemic-hyperinsulinemic clamps and biopsies of vastus lateralis muscle were performed. In 10 subjects, additional biopsies were taken after a 4-h clamp and after a clamp with concurrent Intralipid/heparin infusion. We identified 13 ceramides and sphingomyelins according to fatty acid residues. Insulin sensitivity was related to total ceramide content ($r = -0.49$, $P = 0.01$) and to ceramide consisting of palmitic ($r = -0.48$, $P = 0.011$), palmitoleic ($r = -0.45$, $P = 0.019$), mirystic ($r = -0.42$, $P = 0.028$), and nervonic acid ($r = -0.39$, $P = 0.047$). Hyperinsulinemia did not affect estimated muscle parameters. Intralipid/heparin infusion resulted in a 24.73% decrease in insulin sensitivity ($P = 0.007$) and a 47.81% increase in ceramide content ($P = 0.005$). These changes were significantly related to each other ($r = -0.64$, $P = 0.046$). A relationship with the decrease in insulin sensitivity was also observed for ceramides consisting of palmitic ($r = -0.68$, $P = 0.03$) and linoleic ($r = -0.66$, $P = 0.038$) acid. Our data indicate that the sphingomyelin signaling pathway in muscle might be an important factor determining the development of insulin resistance in humans. *Diabetes* 53:1215–1221, 2004

Insulin resistance is a key factor in the pathogenesis of type 2 diabetes (1), and it is also connected with greater cardiovascular risk (2). Skeletal muscles are the important site of insulin action; decreased insulin-stimulated muscle glucose uptake is one of the mechanisms responsible for the development of insulin resistance (3). Intramyocellular lipid accumulation might contribute to an impairment in insulin action. It was demonstrated that insulin sensitivity was negatively related to skeletal muscle triglyceride content (4–6), and it was also dependent on the fatty acid composition of muscle phospholipids (7,8).

Another important intracellular lipid pool is associated with the sphingomyelin signaling pathway. Sphingomyelin is a sphingolipid, located mostly in the outer layer of the plasma membrane. It is hydrolyzed by the enzyme Mg^{2+}-dependent neutral sphingomyelinase to phosphorylcholine and ceramide. Ceramide is the second messenger in the sphingomyelin signaling pathway. Some amount of ceramide might also come from hydrolysis of lysosomal and endosomal sphingomyelin (by acid sphingomyelinase) and from de novo synthesis (from serine and palmitoyl-CoA). The key intermediate in the de novo pathway is sphinganine. Ceramide is hydrolyzed by the enzyme ceramidase to sphingosine and long-chain fatty acid (9–11).

Experimental studies revealed that ceramide might impair insulin action. Ceramide might interfere with the insulin signaling pathway through maintaining protein kinase B (PKB)/Akt in an inactive dephosphorylated state (12,13). A further consequence of ceramide action is the reduction of GLUT4 translocation to plasma membrane and a decrease in insulin-stimulated glucose uptake (14).

Formation of ceramide might also be an important step in the insulin-desensitizing action of inflammatory cytokines. Experimental studies revealed that tumor necrosis factor (TNF)-α, a well-known mediator of insulin resistance, acts through activation of neutral sphingomyelinase and induction of ceramide formation (15,16). Incubation of adipocytes with cell-permeable ceramides mimicked some effects of TNF-α (17). Also, inhibition of ceramide generation reversed TNF-α–induced insulin resistance (18).

It was demonstrated that rat skeletal muscle contains different sphingomyelins and ceramides according to fatty acid residue, with the highest content in muscles with the

greatest oxidative potential (10). However, there is only a little in vivo data about ceramide content in human skeletal muscle, and it remains unclear whether muscle ceramide might determine whole-body insulin action (19).

The aim of the present study was to examine the content and composition of fatty acids in ceramide and sphingomyelin in human skeletal muscle and to evaluate their relationships with insulin sensitivity and their regulation by insulin and lipid infusions.

RESEARCH DESIGN AND METHODS

The study was conducted on 27 healthy male subjects aged 20–40 years. All participants had no ischemic heart disease, hypertension, peripheral vascular disease, infections, or any other serious medical problems. Before the study, physical examination and appropriate laboratory tests were performed. All subjects underwent an oral glucose tolerance test, and they all had normal glucose tolerance according to World Health Organization criteria (20). Subjects included in the present study were nonsmokers and were not taking drugs known to affect carbohydrate or lipid metabolism. All analyses were performed after an overnight fast. The study protocol was approved by the ethics committee of the Medical University, Białystok, Poland. All subjects gave written informed consent before entering the study.

Anthropometry. BMI was calculated as body weight in kilograms divided by height in meters squared (kg/m^2). The waist-to-hip ratio (WHR) was estimated. Percent of body fat was assessed by bioelectric impedance analysis using the Tanita TBF-511 body fat analyzer (Tanita, Tokyo).

Insulin sensitivity. Insulin sensitivity was measured with the euglycemic-hyperinsulinemic clamp technique, according to DeFronzo et al. (21). On the morning of the study, two venous catheters were inserted into antecubital veins, one for the infusion of insulin and glucose and the other in the contralateral hand for blood sampling, with that hand heated to ~60°C. Insulin (Actrapid HM; Novo Nordisk, Copenhagen, Denmark) was given as a primed-continuous intravenous infusion for 240 min at 40 mU $\cdot$ m^{-2} $\cdot$ min^{-1}, resulting in constant hyperinsulinemia of ~550 pmol/l. Arterialized blood glucose was obtained every 5 min, and 20% dextrose (1.11 mol/l) infusion was adjusted to maintain plasma glucose levels at 5.0 mmol/l. The rate of whole-body glucose uptake (M value) was calculated as the mean glucose infusion rate during the last 40 min of the clamp, normalized for fat-free mass.

Additionally, another clamp, with concurrent Intralipid/heparin infusion, was performed in 10 subjects. The experiment was carried out within 1 week from the first clamp, with 20% Intralipid (Fresenius Kabi, Uppsala, Sweden) given at 0.013 ml $\cdot$ kg^{-1} $\cdot$ min^{-1} and heparin given at 0.2 units $\cdot$ kg^{-1} $\cdot$ min^{-1}. Intralipid/heparin infusion was started 1 h before the beginning of the clamp and maintained throughout the study period. Intralipid was given until the end of the study, whereas heparin was stopped 30 min before the end of the clamp.

Other blood analyses. Fasting blood samples were also taken from the antecubital vein before the beginning of the clamp for the determination of plasma lipids, TNF-α, and soluble forms of TNF-α receptors (sTNFR1 and sTNFR2). Samples were frozen at −70°C for the determination of the plasma TNF-α system.

Muscle biopsies. In each subject before the clamp, a percutaneous biopsy of vastus lateralis muscle was performed with a skeletal muscle biopsy needle of 4.5 mm diameter (Popper & Sons, New Hyde Park, NY) (22). Biopsy was taken ~15 cm above the patella, using local anesthesia with 1% lidocaine, after a small skin incision of ~1 cm. In 10 individuals, two additional biopsies were obtained, the second one after a 4-h clamp and the third one after a clamp with Intralipid/heparin infusion.

Muscles were immediately frozen in liquid nitrogen and were kept at −70°C until analyses. To avoid contamination of extracellular fat (even in small amounts), muscle fibers were isolated and lyophilized in liquid nitrogen before analyses.

Analysis of sphingomyelin signaling pathway in muscle. Muscle ceramides and sphingomyelins were assayed as described previously (10). Lipids were extracted according to the method of Folch et al. (23) in chloroform–methanol (2:1 vol/vol) with an addition of butylated hydroxytoluene (Sigma-Aldrich, St. Louis, MO) as an antioxidant, in a dose of 30 mg per 100 ml. Ceramides and sphingomyelins were separated with thin-layer chromatography on silica gel plates (0.22 mm Kieselgel 60; Merck, Darmstadt, Germany). To isolate ceramide, samples were developed to one-third of the total length of the plate in chloroform–methanol–25% NH_3 (20:5:0.2, vol/vol/vol). The plates were dried and rechromatographed in heptan–isopropyl ether–acetic acid (60:40:3, vol/vol/vol). To isolate sphingomyelin, lipids were fractionated on the plates with chloroform–methanol–acetic acid–water (50:37.5:3.5:2, vol/vol/vol/vol) as the developing solvent. Standards of ceramide (Sigma) and

sphingomyelin (Sigma) were run along with the samples. After ceramide and sphingomyelin separation, fatty acids, together with methylpentadecanoic acid (Sigma) used as an internal standard, were transmethylated in the presence of 1 ml of 14% boron fluoride in methanol at 100°C for 90 min (24). The samples were cooled to room temperature, and 1 ml of pentane and 0.5 ml of water were added. After centrifugation, the upper pentane phase was dried under nitrogen. The methyl esters were dissolved in 40 μl of hexane and analyzed by gas-liquid chromatography. A Hewlett-Packard 5890 Series II and a fused HP-INNOWax (50-m) capillary column were used. Injector and detector temperatures were set at 250°C each. The oven temperature was increased linearly from 160 to 230°C at a rate of 5°C/min. Individual fatty acid methyl esters were quantified using the area corresponding to the internal standards (Sigma). Total ceramide and sphingomyelin content was estimated as the sum of the particular fatty acid content of the assessed fraction and was expressed in nanomoles per gram of tissue.

Muscle activity of enzymes, membrane Mg^{2+}-dependent neutral sphingomyelinase, and lysosomal Zn^{2+}-independent acid sphingomyelinase was measured as described by Liu et al. (25). Briefly, lyophilized muscles were homogenized in 300 μl 20 mmol/l Tris-HCl, ph 7.4, with 0.1% Triton X-100, 1 mmol/l phenylmethylsulfonyl fluoride, and Protease Inhibitor Cocktail (Sigma) at a dose of 1.2 μl/ml of buffer. Samples were then centrifuged at 3,000g for 10 min, and 50 μl of supernatant was used for analysis. The activity of both sphingomyelinases was measured using radiolabeled substrate, [N-choline-methyl-^{14}C]-sphingomyelin (PerkinElmer Life Sciences, Boston, MA). For neutral sphingomyelinase, the reaction mixture contained 100 nmol sphingomyelin (1,154 dpm/nmol sphingomyelin) in 100 mmol/l Tris, pH 7.4, with 0.1% Triton X-100, 5 mmol/l $MgCl_2$, and 5 mmol/l dithiothreitol in a final volume of 200 μl. For acid sphingomyelinase, the reaction mixture contained 100 nmol sphingomyelin (1,154 dpm/nmol sphingomyelin) in 100 mmol/l sodium acetate, pH 5.0, with 0.1% Triton X-100. The reaction product, [N-choline-methyl-^{14}C]-phosphocholine, was mixed with 5 ml of scintillation solution for radioactivity counting. Sample protein content was estimated with BCA protein assay (Sigma). Enzyme activity was expressed in nanomoles of ceramide generated per 1 h per mg of protein in supernatant.

Muscle sphingosine and sphinganine assay was described previously (11). In brief, after lipid extraction, sphingosine and sphinganine were identified and quantified with high-performance liquid chromatography (HPLC). A LaChrom D-7000 HPLC (Hitachi) and Merck LichroCART 250-4 RP-18 (5 μm) column were used. The solvent system was methanol/5 mmol/l potassium phosphate, pH 7.0 (9:1 vol/vol) with a flow rate of 1.25 ml/min. The fractions were identified using a Merck LaChrom L-7480 fluorescence detector (λ_{ex} = 340 nm, λ_{em} = 455 nm) according to the retention time of sphigosine and sphinganine. The data were analyzed according to previously obtained curves for the standards of sphingosine and sphinganine. D-700 HPLC System Manager software was used.

Other analytical procedures. Plasma glucose was measured immediately by the enzymatic method using a 2300 STAT Plus glucose analyzer (YSI, Yellow Springs, OH). Plasma insulin was measured with a Medgenix EASIA test (BioSource Europe, Nivelles, Belgium). The minimum detectable concentration was 1.05 pg/l, and the intra- and interassay coefficients of variation (CVs) were <5.5 and <10%, respectively. With that method, human and animal pro-insulins present no cross-reaction. Plasma total cholesterol, HDL cholesterol, and triglycerides were assessed by enzymatic methods (Cormay, Warsaw, Poland), and LDL cholesterol was calculated from Friedewald's formula. Plasma free fatty acids (FFAs) were measured by the colorimetric method (26).

Plasma TNF-α concentrations were measured with the ultrasensitive ELISA kit (BioSource International, Camarillo, CA) with the minimum detectable concentration <0.09 pg/ml and with the intra- and interassay CVs <6.8 and <10.0%, respectively. Plasma sTNFR1 and sTNFR2 were determined with EASIA kits (BioSource Europe). The minimum detectable concentration was 0.05 ng/ml for sTNFR1 and 0.1 ng/ml for sTNFR2. The intra- and interassay CVs for both receptors were <6.5 and <9%, respectively. sTNFR1 EASIA does not cross-react with sTNFR2, and TNF-α does not interfere with the assay.

Statistical analysis. The statistics were performed with Statistica 5.0 software (StatSoft, Krakow, Poland). Relationships between variables were estimated with the simple and multiple regression analysis. The difference between baseline values and the results obtained after insulin or Intralipid/heparin infusions were assessed with Wilcoxon's rank-sum test. The level of significance was accepted at P value <0.05.

RESULTS

Baseline values. Clinical characteristics of the study group are given in Table 1. We identified 13 different ceramides and sphingomyelins in muscle, according to particular fatty acid residues (Table 2). Ceramide–fatty

TABLE 1
Clinical characteristics of the study group ($n = 27$)

Age (years)	26.07 ± 6.03
BMI (kg/m^2)	24.53 ± 4.13
WHR	0.82 ± 0.07
Percent of body fat	19.24 ± 7.99
Fasting plasma glucose (mmol/l)	4.97 ± 0.58
Fasting plasma insulin (pmol/l)	73.37 ± 44.53
M (μmol $\cdot$ min^{-1} $\cdot$ kg fat-free mass^{-1})	53.67 ± 19.80
Plasma FFA (mmol/l)	0.54 ± 0.21
Total cholesterol (mmol/l)	4.67 ± 0.88
Triglycerides (mmol/l)	1.20 ± 0.88
HDL cholesterol (mmol/l)	1.35 ± 0.30
LDL cholesterol (mmol/l)	2.82 ± 0.82
TNF-α (pg/l)	2.47 ± 2.39
sTNFR1 (ng/ml)	1.79 ± 0.55
sTNFR2 (ng/ml)	5.61 ± 1.34

Data are expressed as means $\pm$ SD.

TABLE 2
Muscle ceramide and sphingomyelin content in the study group ($n = 27$)

Fatty acid	Ceramide (nmol/g tissue)	Sphingomyelin (nmol/g tissue)
Total	499.81 ± 266.81	$1,334.75 \pm 246.30$
Myristic (14:0)	49.52 ± 32.70	49.47 ± 25.55
Palmitic (16:0)	153.76 ± 104.14	379.29 ± 103.15
Palmitoleic (16:1)	13.33 ± 10.56	4.44 ± 5.25
Stearic (18:0)	97.90 ± 60.49	391.34 ± 59.93
Oleic (18:1)	88.21 ± 59.98	27.98 ± 11.13
Linoleic (18:2)	24.61 ± 16.38	22.24 ± 12.40
Linolenic (18:3)	4.25 ± 3.77	1.59 ± 3.06
Arachidic (20:0)	7.42 ± 5.36	37.49 ± 9.68
Arachidonic (20:4)	18.65 ± 25.95	12.92 ± 3.94
Eicosapentaenoic (20:5)	1.69 ± 2.38	1.05 ± 1.91
Behenic (22:0)	9.86 ± 8.69	116.65 ± 33.89
Docosahexaenoic (22:6)	1.62 ± 2.70	1.85 ± 3.46
Nervonic (24:1)	28.98 ± 30.48	288.44 ± 92.55

Data are expressed as means $\pm$ SD.

acid consisted of 64.06 ± 9.32% saturated fatty acids (SFAs), 25.89 ± 7.76% monounsaturated fatty acids (MUFAs), and 10.05 ± 2.59% polyunsaturated fatty acids (PUFAs), whereas sphingomyelin–fatty acid consisted of 73.20 ± 5.37% SFAs, 23.83 ± 5.38% MUFAs, and 2.97 ± 1.05% PUFAs.

We observed a significant negative correlation between muscle total ceramide content and insulin sensitivity ($r = -0.49$, $P = 0.01$) (Fig. 1). The relationship remained significant when we analyzed it separately for ceramide-SFA ($r = -0.47$, $P = 0.014$), ceramide-MUFA ($r = -0.40$, $P = 0.038$), and ceramide-PUFA ($r = -0.41$, $P = 0.034$). For individual fatty acids, ceramide consisting of palmitic acid was most strongly associated with insulin sensitivity ($r = -0.48$, $P = 0.011$); the relationship was also significant for ceramide consisting of palmitoleic acid ($r = -0.45$, $P = 0.019$), mirystic acid ($r = -0.42$, $P = 0.028$), and nervonic acid ($r = -0.39$, $P = 0.047$). However, when we expressed particular ceramide fatty acid as a percentage of total ceramide content, there was no correlation between insulin sensitivity and percentage of any individual fatty acids in ceramide. Multiple regression analysis revealed that correlation between total ceramide and insulin sensitivity was independent of BMI, WHR, percent of body fat, fasting plasma glucose, insulin, FFAs, cholesterol, and triglycerides ($\beta = -0.59$, $P = 0.008$) and that muscle ceramide was responsible for 24% of M value variability ($P = 0.0095$). There were no significant correlations between muscle ceramide and anthropometric measurements (BMI: $r = 0.19$, $P = 0.33$; WHR: $r = 0.08$, $P = 0.68$; percent of body fat: $r = 0.15$, $P = 0.47$).

In contrast, marked correlations between muscle total sphingomyelin content and anthropometric parameters were observed (BMI: $r = 0.46$, $P = 0.017$; WHR: $r = 0.36$, $P = 0.069$, NS; percent of body fat: $r = 0.42$, $P = 0.03$), whereas there was no association between sphingomyelin and insulin sensitivity ($r = 0.06$, $P = 0.78$).

The activity of muscle membrane Mg^{2+}-dependent neutral sphingomyelinase was 0.70 ± 0.21 nmol of ceramide $\cdot$ h^{-1} $\cdot$ mg of protein^{-1}, and the activity of lysosomal Zn^{2+}-independent acid sphingomyelinase was 3.16 ± 0.83 nmol of ceramide $\cdot$ h^{-1} $\cdot$ mg of protein^{-1}. The activities of sphingomyelinases were not related to insulin sensitivity ($r = -0.21$, $P = 0.30$ and $r = -0.15$, $P = 0.46$ for neutral

and acid sphingomyelinase, respectively). Neutral sphingomyelinase was associated with total ceramide ($r = 0.38$, $P = 0.048$), and for acid sphingomyelinase that association was of borderline significance ($r = 0.34$, $P = 0.082$). Additionally, an inverse correlation between neutral sphingomyelinase and sTNFR1 was found ($r = -0.38$, $P = 0.049$). It was the only significant correlation between the TNF-α system and estimated muscle parameters.

Muscle sphingosine content was 0.94 ± 0.15 nmol/g tissue and sphinganine 0.31 ± 0.09 nmol/g tissue. Both sphingosine and sphinganine were markedly related to insulin sensitivity ($r = -0.41$, $P = 0.033$ and $r = -0.56$, $P = 0.002$, respectively). Correlation between total ceramide and sphinganine was of borderline significance ($r = 0.35$, $P = 0.072$).

Effect of 4-h hyperinsulinemia. The 4-h hyperinsulinemia, obtained during the clamp, did not affect estimated parameters of sphingomyelin pathway in muscle (Tables 3–5).

Intralipid/heparin infusion. Intralipid/heparin infusion, administered during the clamp, resulted in an increase in plasma FFAs from 0.56 ± 0.22 baseline to 1.75 ± 0.69 mmol/l ($P = 0.0069$). This was accompanied by a reduction in insulin sensitivity of 24.73% (from 53.42 ± 21.28 to 40.21 ± 22.93 μmol $\cdot$ min^{-1} $\cdot$ kg fat-free mass^{-1}, $P = 0.007$).

After Intralipid/heparin infusion, we observed a 47.81% increase in muscle total ceramide content ($P = 0.005$) (Table 3). The increase was mostly attributable to the changes in ceramide–palmitic acid ($P = 0.005$) and cera-
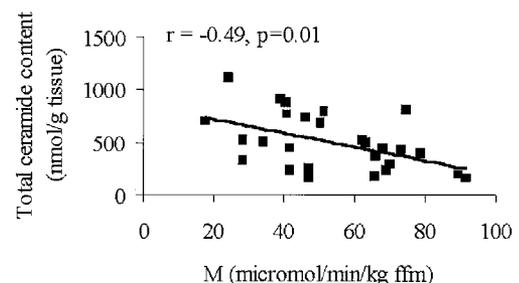

FIG. 1. Relationship between insulin sensitivity (M value) and total ceramide content in the studied group. ffm, fat-free mass.

TABLE 3
Skeletal muscle ceramide content (nmol/g tissue) at baseline, after 4-h hyperinsulinemia, and after clamp with Intralipid/heparin infusion ($n = 10$)

Fatty acid	Baseline	After 4-h clamp	After 4-h clamp with Intralipid/heparin infusion
n	10	10	10
Total	437.66 ± 263.50	423.76 ± 130.67	646.89 ± 311.43*
Myristic (14:0)	38.16 ± 11.74	43.70 ± 29.41	55.53 ± 30.24
Palmitic (16:0)	133.30 ± 81.94	145.38 ± 48.68	209.64 ± 95.81*
Palmitoleic (16:1)	9.78 ± 8.37	8.47 ± 4.24	10.34 ± 6.49
Stearic (18:0)	96.47 ± 69.69	97.61 ± 43.68	149.52 ± 105.59*
Oleic (18:1)	74.39 ± 60.65	53.70 ± 42.33	92.48 ± 66.64
Linoleic (18:2)	20.92 ± 16.34	13.15 ± 7.34	28.52 ± 20.09*
Linolenic (18:3)	5.58 ± 4.97	4.93 ± 2.64	8.92 ± 4.45*
Arachidic (20:0)	7.66 ± 6.11	7.36 ± 4.28	9.96 ± 5.94
Arachidonic (20:4)	7.42 ± 7.98	5.88 ± 5.97	6.07 ± 8.41
Eicosapentaenoic (20:5)	2.43 ± 2.12	3.91 ± 2.71	4.99 ± 1.78*
Behenic (22:0)	12.01 ± 10.06	13.32 ± 9.41	21.94 ± 11.62*
Docosahexaenoic (22:6)	3.55 ± 3.45	3.64 ± 3.64	9.43 ± 4.66*
Nervonic (24:1)	25.98 ± 16.10	22.70 ± 13.41	39.56 ± 20.68*

Data are expressed as means ± SD. *$P < 0.05$ in comparison to baseline values.

mide–stearic acid ($P = 0.016$) and also reached the level of significance for a part of other individual fatty acids in ceramide (Table 3). A significant negative relationship was found between the decrease in insulin sensitivity and the concurrent increase in total ceramide content ($r = -0.64$, $P = 0.046$), i.e., the greater the increase in ceramide, the greater the decrease in M value. For individual fatty acids, the decrease in insulin sensitivity was markedly related to the increase in ceramide–palmitic acid ($r = -0.68$, $P = 0.03$) and ceramide–linoleic acid ($r = -0.66$, $P = 0.038$).

Another significant difference observed after Intralipid/heparin infusion was a 15.49% increase in muscle total sphingomyelin content ($P = 0.028$). As in ceramide, it was mostly attributable to the changes in sphingomyelin–palmitic acid and sphingomyelin–stearic acid (both $P = 0.017$), with a concurrent increase in part of other individual fatty acids in sphingomyelin (Table 4).

Finally, we observed a marked increase of 18.15% ($P = 0.022$) in acid sphingomyelinase activity and of 12.90%

($P = 0.028$) in sphinganine content after Intralipid/heparin infusion in comparison to baseline values (Table 5). The slight increase in sphingosine content was not significant ($P = 0.14$). The increase in total ceramide was related to an increase in acid sphingomyelinase ($r = 0.64$, $P = 0.047$), whereas its relationship with the concurrent increase in sphinganine was of borderline significance ($r = 0.59$, $P = 0.072$).

DISCUSSION

Since the study by Randle et al. (27) was reported, it was supposed that FFA influx results in increased lipid oxidation and decreased glucose utilization. The so-called "glucose–fatty acid cycle" was the proposed mechanism for the development of lipid-induced insulin resistance. However, recent years provided evidence that in insulin-resistant states, tissue lipid oxidation is decreased and there is a shift toward an increased lipid storage (28). It was

TABLE 4
Skeletal muscle sphingomyelin content (nmol/g tissue) at baseline, after 4-h hyperinsulinemia, and after clamp with Intralipid/heparin infusion ($n = 10$)

Fatty acid	Baseline	After 4-h clamp	After 4-h clamp with Intralipid/heparin infusion
n	10	10	10
Total	1,281.52 ± 182.90	1,327.93 ± 258.66	1,479.99 ± 265.89*
Myristic (14:0)	38.41 ± 8.35	40.52 ± 10.99	43.89 ± 17.57
Palmitic (16:0)	346.38 ± 57.26	387.44 ± 90.60	436.51 ± 98.28*
Palmitoleic (16:1)	3.01 ± 1.23	2.58 ± 1.65	4.47 ± 1.86
Stearic (18:0)	400.63 ± 62.39	395.75 ± 58.84	436.54 ± 74.08*
Oleic (18:1)	21.35 ± 3.60	25.53 ± 10.12	31.52 ± 13.12*
Linoleic (18:2)	17.36 ± 4.44	21.18 ± 8.89	25.10 ± 6.99*
Linolenic (18:3)	2.97 ± 3.66	3.85 ± 3.49	6.49 ± 7.23*
Arachidic (20:0)	34.50 ± 10.46	35.06 ± 8.80	38.81 ± 9.89
Arachidonic (20:4)	11.13 ± 3.09	11.79 ± 5.89	13.34 ± 4.01
Eicosapentaenoic (20:5)	1.60 ± 1.83	3.05 ± 2.02	4.28 ± 1.93*
Behenic (22:0)	113.96 ± 25.83	118.49 ± 27.89	131.73 ± 30.35
Docosahexaenoic (22:6)	2.91 ± 3.18	3.86 ± 2.85	6.23 ± 1.56*
Nervonic (24:1)	287.31 ± 70.83	278.81 ± 85.57	301.10 ± 69.94

Data are expressed as means ± SD. *$P < 0.05$ in comparison to baseline values.

TABLE 5
Muscle membrane Mg^{2+}-dependent neutral sphingomyelinase and lysosomal Zn^{2+}-independent acid sphingomyelinase activities and sphingosine and sphinganine content at baseline, after 4-h hyperinsulinemia, and after clamp with Intralipid/heparin infusion ($n = 10$)

	Baseline	After 4-h clamp	After 4-h clamp with Intralipid/heparin infusion
	10	10	10
Neutral sphingomyelinase (nmol of ceramide $\cdot h^{-1} \cdot$ mg of protein^{-1})	0.53 ± 0.18	0.44 ± 0.16	0.48 ± 0.14
Acid sphingomyelinase (nmol of ceramide $\cdot h^{-1} \cdot$ mg of protein^{-1})	2.92 ± 0.40	3.01 ± 0.68	3.45 ± 0.57*
Sphingosine (nmol/g tissue)	0.95 ± 0.16	0.98 ± 0.12	1.08 ± 0.15
Sphinganine (nmol/g tissue)	0.31 ± 0.06	0.30 ± 0.08	0.35 ± 0.04*

Data are expressed as means $\pm$ SD *$P < 0.05$ in comparison to baseline values.

demonstrated that FFAs induced insulin resistance in humans through inhibition of glucose transport activity (29), and it was supposed that intramuscular accumulation of fatty acids, or their metabolites, played an important role in the pathogenesis of human insulin resistance (30).

In the present study we demonstrated, for the first time to our knowledge, an association between skeletal muscle ceramide content and insulin resistance in humans. Muscle ceramide was not related to the measurements of adiposity. Similar relationships were reported previously for muscle triglycerides (4). Previously, it was demonstrated that insulin-resistant obese Zucker rats had higher levels of muscle ceramide in comparison to lean controls (31), and mice overexpressing muscle lipoprotein lipase develop insulin resistance with the concurrent muscle ceramide accumulation (32). As mentioned, experimental findings demonstrated that ceramide impaired insulin signaling through inactivation of PKB/Akt (12,13). Ceramide might inactivate PKB/Akt through acceleration of the enzyme dephosphorylation by protein phosphatase 2A (12,13, 33) or through blocking of insulin-stimulated translocation of Akt/PKB to plasma membrane (34). Experimental studies linked ceramide action with impaired insulin signaling and GLUT4 translocation within a single examined tissue. In the present study, an association was found between skeletal muscle ceramide content and whole-body insulin action. Furthermore, we found that muscle ceramide was negatively associated with insulin sensitivity independently of any measurements of obesity, plasma lipids, glucose, and insulin. Thus, our data show that muscle ceramide accumulation might be a clinically significant finding, important for the development of insulin resistance. Probably, for the decrease in insulin action, total ceramide content is more important than specific ceramide fatty acid composition.

Total muscle ceramide was related to neutral sphingomyelinase activity, and correlations with acid sphingomyelinase and sphinganine were of borderline significance. These data suggest indirectly that muscle ceramide content might be the result of complex regulation of sphingomyelin hydrolysis and de novo synthesis pathways. Ceramide level might also be regulated by the rate of hydrolysis to sphingosine and fatty acid. These findings might explain the fact that muscle ceramides and sphingomyelins were related to clinical parameters in a different manner.

Both sphinganine (intermediate in de novo synthesis) and sphingosine (product of ceramide degradation) were negatively associated with insulin sensitivity. This might simply reflect an association of both factors with ceramide metabolism. However, it should be noted that sphinganine and sphingosine are also biologically active compounds,

able to inhibit insulin-stimulated 2-deoxyglucose uptake in incubated rat soleus muscle (35). It is therefore possible that observed relationships reflect an independent mechanism by which both sphinganine and sphingosine affect insulin action.

Ceramide is also the proposed messenger in TNF-α insulin-desensitizing action (15–18). Skeletal muscle TNF-α expression is associated with insulin resistance (36), and it is believed that circulating soluble forms of TNF-α receptors, especially sTNFR2, reflect local action of the cytokine in tissues (37). Previous studies of Fernandez-Real and colleagues (38,39) and our studies (40–42) suggested indirectly that muscle might be an important source of sTNFRs. If we recognize ceramide as the cellular TNF-α target, findings of the present study (i.e., lack of significant correlations between muscle ceramide and circulating TNF-α system) do not support the hypothesis about sTNFRs as indicators of auto- and paracrine TNF-α action in muscle. The only correlation we found was a negative relationship between sTNFR1 and neutral sphingomyelinase, an enzyme activated by TNF-α (15,16). This might indicate that sTNFR1 might serve rather as an inhibitory factor for some cytokine actions.

Acute increase in plasma FFA concentrations, obtained during clamp with Intralipid/heparin infusion, resulted in a 24.73% decrease in insulin sensitivity. These data are similar to the values reported by other authors (43). The decrease in insulin sensitivity was inversely related to the concurrent increase in muscle ceramide. Changes in ceramide content and in other estimated muscle parameters might be attributable to an elevation in plasma FFA because hyperinsulinemia itself did not affect muscle lipids.

Mechanisms of fatty acid–induced insulin resistance have been widely studied. It was demonstrated that acute elevation in plasma FFAs resulted in impairment in tyrosine phosphorylation of insulin receptor substrate (IRS)-1 and a decrease in IRS-1–associated phosphatidylinositol 3-kinase activity (29,43). Itani et al. (19) found that insulin resistance, developed during lipid infusion, was associated with an increase in diacylglycerol content and protein kinase C activity and a decrease in IκB-α, an inhibitor of nuclear factor-κB, in human muscle. Our study provides an evidence for another potential pathway, i.e., muscle ceramide accumulation, for the decrease in insulin action associated with lipid infusion. It should be noted that our study does not prove any direct causality; we can hypothesize of ceramide role as the causal factor on the basis of previous experimental findings.

Acute ceramide formation after Intralipid/heparin infusion is a novel finding of the present study. In the study of

Itani et al. (19), no change in muscle ceramide mass after lipid infusion was found. It is difficult to compare these data with ours because the authors did not show the ceramide results (19). No increase in ceramide content after lipid infusion was also found in rat soleus muscle (44). However, we lyophilized the muscle fibers, and this procedure, which eliminates interference of even a small amount of extracellular fat, might allow more precise analysis. The difference between the study by Itani et al. (19) and ours might also come from the analysis of particular fatty acids in ceramide that was performed in our study.

Experimental studies provide evidence that tissue ceramide formation might be, in part, fatty acid dependent. De novo ceramide synthesis from fatty acids and serine was linked with lipoapoptosis in β-cells (45). As mentioned, mice overexpressing tissue-specific lipoprotein lipase exhibit intracellular ceramide accumulation (32), and these data demonstrate that ceramide formation is associated with fatty acid availability. Incubation of C2C12 myotubes with palmitate elevated ceramide level twofold (12). In that study, palmitate inhibited insulin-stimulated phosphorylation of PKB/Akt and glycogen synthase kinase-3; incubation of cells with ceramide closely reproduced these effects (12). In the study by Chavez et al. (46), exposing muscle cells to particular SFAs, but not MUFAs, also inhibited insulin stimulation of PKB/Akt and resulted in ceramide accumulation. Effect of SFAs on PKB/Akt inactivation was negated by preventing de novo ceramide synthesis (46). These data might give a potential explanation for the findings of the present study, i.e., the increase in ceramide after lipid infusion and a relationship with a concurrent decrease in insulin action.

Intralipid/heparin infusion resulted in, together with ceramide accumulation, an increase in sphingomyelin content, acid sphingomyelinase activity, and sphinganine level. This might indicate that enhanced ceramide formation might be the result of complex upregulation of sphingomyelin hydrolysis and de novo pathways by fatty acids. Experimental studies stress the importance of de novo ceramide synthesis in response to SFAs. The difference might come from different study conditions. Intralipid is a mixture of various fatty acids, and therefore its effect is likely to be more complex than that observed after cell incubation with a single particular fatty acid. The effect of fatty acids on tissue lipid metabolism is dependent on their saturation and elongation, with SFAs promoting de novo synthesis (46) and unsaturated fatty acids enhancing sphingomyelin hydrolysis (47). Studies with cells expressing liver fatty acid binding protein revealed that sphingomyelin content might be increased through increased fatty acid influx (48). It was also demonstrated that diacylglycerol, which contains two fatty acid residues, might stimulate acid, but not neutral, sphingomyelinase (49).

In conclusion, we demonstrated that *1*) skeletal muscle ceramide content is inversely related to insulin sensitivity, *2*) acute elevation of plasma FFAs through Intralipid/heparin infusion results in muscle ceramide accumulation, and *3*) the increase in muscle ceramide is related to a concurrent decrease in insulin sensitivity. Our data indicate that the sphingomyelin signaling pathway in muscle might be an important factor determining the development of insulin resistance in humans.

REFERENCES

1. Ferrannini E: Insulin resistance versus insulin deficiency in non-insulin-dependent diabetes mellitus: problems and prospects. *Endocr Rev* 19:477–490, 1998
2. Fernandez-Real JM, Ricart W: Insulin resistance and chronic cardiovascular inflammatory syndrome. *Endocr Rev* 24:278–301, 2003
3. Shulman GI, Rothman DL, Jue T, Stein P, DeFronzo RA, Shulman RG: Quantitation of muscle glycogen synthesis in normal subjects and subjects with non-insulin-dependent diabetes by ^{13}C nuclear magnetic resonance spectroscopy. *N Engl J Med* 322:223–228, 1990
4. Pan DA, Lillioja S, Kriketos AD, Milner MR, Baur LA, Bogardus C, Jenkins AB, Storlien LH: Skeletal muscle triglyceride levels are inversely related to insulin action. *Diabetes* 46:983–988, 1997
5. Jacob S, Machann J, Rett K, Brechtel K, Volk A, Renn W, Maerker E, Matthaei S, Schick F, Claussen CD, Haring HU: Association of increased intramyocellular lipid content with insulin resistance in lean nondiabetic offspring of type 2 diabetic subjects. *Diabetes* 48:1113–1119, 1999
6. Perseghin G, Scifo P, De Cobelli F, Pagliato E, Battezzati A, Arcelloni C, Vanzulli A, Testolin G, Pozza G, Del Maschio A, Luzi L: Intramyocellular triglyceride content is a determinant of in vivo insulin resistance in humans: a 1H–13C nuclear magnetic resonance spectroscopy assessment in offspring of type 2 diabetic parents. *Diabetes* 48:1600–1606, 1999
7. Borkman M, Storlien LH, Pan DA, Jenkins AB, Chisholm DJ, Campbell LV: The relation between insulin sensitivity and the fatty-acid composition of skeletal muscle phospholipids. *N Engl J Med* 328:238–244, 1993
8. Pan DA, Lillioja S, Milner MR, Kriketos AD, Baur LA, Bogardus C, Storlien LH: Skeletal muscle membrane lipid composition is related to adiposity and insulin action. *J Clin Invest* 96:2802–2808, 1995
9. Kolesnick R: The therapeutic potential of modulating the ceramide/sphingomyelin pathway. *J Clin Invest* 110:3–8, 2002
10. Dobrzyn A, Gorski J: Ceramides and sphingomyelins in skeletal muscles of the rat: content and composition: effect of prolonged exercise. *Am J Physiol* 282:E277–E285, 2002
11. Dobrzyn A, Gorski J: Effect of acute exercise on the content of free sphinganine and sphingosine in different skeletal muscle types of the rat. *Horm Metab Res* 34:523–529, 2002
12. Schmitz-Pfeiffer C, Craig DL, Biden TJ: Ceramide generation is sufficient to account for the inhibition of the insulin-stimulated PKB pathway in C2C12 skeletal muscle cells pretreated with palmitate. *J Biol Chem* 274:24202–24210, 1999
13. Teruel T, Hernandez R, Lorenzo M: Ceramide mediates insulin resistance by tumor necrosis factor-α in brown adipocytes by maintaining Akt in an inactive dephosphorylated state. *Diabetes* 50:2563–2571, 2001
14. Summers SA, Garza LA, Zhou H, Birnbaum MJ: Regulation of insulin-stimulated glucose transporter GLUT4 translocation and Akt kinase activity by ceramide. *Mol Cell Biol* 18:5457–5464, 1998
15. Kanety H, Hemi R, Papa MZ, Karasik A: Sphingomyelinase and ceramide suppress insulin-induced tyrosine phosphorylation of the insulin receptor substrate-1. *J Biol Chem* 271:9895–9897, 1996
16. Peraldi P, Hotamisligil GS, Buurman WA, White MF, Spiegelman BM: Tumor necrosis factor (TNF)-α inhibits insulin signalling through stimulation of the p55 TNF receptor and activation of sphingomyelinase. *J Biol Chem* 271:13018–13022, 1996
17. Wang CN, O'Brien L, Brindley DN: Effects of cell-permeable ceramides and tumor necrosis factor-α on insulin signaling and glucose uptake in 3T3–L1 adipocytes. *Diabetes* 47:24–31, 1998
18. Grigsby RJ, Dobrowsky RT: Inhibition of ceramide production reverses TNF-induced insulin resistance. *Biochem Biophys Res Commun* 287:1121–1124, 2001
19. Itani SI, Ruderman NB, Schmieder F, Boden G: Lipid-induced insulin resistance in human muscle is associated with changes in diacylglycerol, protein kinase C, and IκB-α. *Diabetes* 51:2005–2011, 2002
20. Alberti KG, Zimmet PZ: Definition, diagnosis and classification of diabetes mellitus and its complications. Part 1. Diagnosis and classification of diabetes mellitus: provisional report of a WHO consultation. *Diabet Med* 15:539–553, 1998
21. DeFronzo RA, Tobin JD, Andres R: Glucose clamp technique: a method for

quantifying insulin secretion and resistance. *Am J Physiol* 237:E214–E223, 1979

22. Bergstrom J: Muscle electrolytes in man. *Scand J Clin Lab Invest* 14 (Suppl. 68):1–110, 1962

23. Folch J, Lees M, Stanley GHS: A simple method for the isolation and purification of total lipids from animal tissues. *J Biol Chem* 226:497–509, 1957

24. Morrison WR, Smith LM: Preparation of fatty acid methyl esters and dimethylacetals from lipids with boron fluoride-methanol. *J Lipid Res* 5:600–608, 1964

25. Liu B, Hassler DF, Gary KS, Weaver K, Hannun YA: Purification and characterization of a membrane bound neutral pH optimum magnesium-dependent and phosphatidylserine-stimulated sphingomyelinase from rat brain. *J Biol Chem* 273:34472–34479, 1998

26. Duncombe WS: The colorimetric microdetermination of nonesterified fatty acids in plasma. *Clin Chim Acta* 9:122–135, 1964

27. Randle PJ, Garland PB, Hales CN, Newsholme EA: The glucose-fatty acid cycle; its role in insulin sensitivity and the metabolic disturbances of diabetes mellitus. *Lancet* i:785–789, 1963

28. Kelley DE, Mandarino LJ: Fuel selection in human skeletal muscle: a reexamination (Review). *Diabetes* 49:677–683, 2000

29. Dresner A, Laurent D, Mercucci M, Griffin ME, Dufour S, Cline GW, Slezak LA, Andersen DK, Hundal RS, Rothman DL, Petersen KF, Shulman GI: Effects of free fatty acids on glucose transport and IRS-1-associated phosphatidylinositol 3-kinase activity. *J Clin Invest* 103:253–259, 1999

30. Shulman GI: Cellular mechanisms of insulin resistance. *J Clin Invest* 106:171–176, 2000

31. Turinsky J, O'Sullivan D, Bayly BP: 1,2-Diacylglycerol and ceramide levels in insulin-resistant tissues of the rat in vivo. *J Biol Chem* 265:16880–16885, 1990

32. Kim JK, Fillmore JJ, Chen J, Yu C, Moore IK, Pypaert M, Lutz EP, Kako Y, Velez-Carrasco W, Goldberg IJ, Breslow JL, Shulman GI: Tissue-specific overexpression of lipoprotein lipase causes tissue-specific insulin resistance. *Proc Natl Acad Sci U S A* 98:7522–7527, 2001

33. Salinas M, Lopez-Valdaliso R, Martin D, Alvarez A, Cuadrado A: Inhibition of PKB/Akt1 by C2-ceramide involves activation of ceramide-activated protein phosphatase in PC12 cells. *Mol Cell Neurosci* 15:156–169, 2000

34. Hajduch E, Balendran A, Batty IH, Litherland GJ, Blair AS, Downes CP, Hundal HS: Ceramide impairs the insulin-dependent membrane recruitment of protein kinase B leading to a loss in downstream signaling in L6 skeletal muscle cells. *Diabetologia* 44:173–183, 2001

35. Turinsky J, Nagel GW: Effect of sphingoid bases on basal and insulin-stimulated 2-deoxyglucose transport in skeletal muscle. *Biochem Biophys Res Commun* 188:358–364, 1992

36. Saghizadeh M, Ong JM, Garvey WT, Henry RR, Kern PA: The expression of TNFα by human muscle: relationship to insulin resistance. *J Clin Invest* 97:1111–1116, 1996

37. Hotamisligil GS, Arner P, Atkinson RL, Spiegelman BM: Differential regulation of the p80 tumor necrosis factor receptor in human obesity and insulin resistance. *Diabetes* 46:451–455, 1997

38. Fernandez-Real JM, Broch M, Ricart W, Casamitjana R, Gutierrez C, Vendrell J, Richart C: Plasma levels of the soluble fraction of tumor necrosis factor receptor 2 and insulin resistance. *Diabetes* 47:1757–1762, 1998

39. Fernandez-Real JM, Molina A, Broch M, Ricart W, Gutierrez C, Casamitjana R, Vendrell J, Soler J, Gomez-Saez JM: Tumor necrosis factor system activity is associated with insulin resistance and dyslipidemia in myotonic dystrophy. *Diabetes* 48:1108–1112, 1999

40. Straczkowski M, Kowalska I, Dzienis-Straczkowska S, Stepien A, Skibinska E, Szelachowska M, Kinalska I: Changes in tumor necrosis factor-α system and insulin sensitivity during an exercise training program in obese women with normal and impaired glucose tolerance. *Eur J Endocrinol* 145:273–280, 2001

41. Straczkowski M, Kowalska I, Stepien A, Dzienis-Straczkowska S, Szelachowska M, Kinalska I: Increased plasma soluble tumor necrosis factor-α receptor 2 level in lean nondiabetic offspring of type 2 diabetic subjects. *Diabetes Care* 25:1824–1828, 2002

42. Dzienis-Straczkowska S, Straczkowski M, Szelachowska M, Stepien A, Kowalska I, Kinalska I: Soluble tumor necrosis factor-α receptors in young obese subjects with normal and impaired glucose tolerance. *Diabetes Care* 26:875–880, 2003

43. Kruszynska YT, Worrall DS, Ofrecio J, Frias JP, Macaraeg G, Olefsky JM: Fatty acid-induced insulin resistance: decreased muscle PI3K activation but unchanged Akt phosphorylation. *J Clin Endocrinol Metab* 87:226–234, 2002

44. Yu C, Chen Y, Cline GW, Zhang D, Zong H, Wang Y, Bergeron R, Kim JK, Cushman SW, Cooney GJ, Atcheson B, White MF, Kraegen EW, Shulman GI: Mechanism by which fatty acids inhibit activation of insulin receptor substrate-1 (IRS-1)-associated phosphatidylinositol 3-kinase activity in muscle. *J Biol Chem* 277:50230–50236, 2002

45. Shimabukuro M, Higa M, Zhou YT, Wang MY, Newgard CB, Unger RH: Lipoapoptosis in beta-cells of obese prediabetic fa/fa rats. Role of serine palmitoyltransferase overexpression. *J Biol Chem* 273:32487–32490, 1998

46. Chavez JA, Knotts TA, Wang LP, Li G, Dobrowsky RT, Florant GL, Summers SA: A role for ceramide, but not diacylglycerol, in the antagonism of insulin signal transduction by saturated fatty acids. *J Biol Chem* 278:10297–10303, 2003

47. Worgall TS, Johnson RA, Seo T, Gierens H, Deckelbaum RJ: Unsaturated fatty acid-mediated decreases in sterol regulatory element-mediated gene transcription are linked to cellular sphingolipid metabolism. *J Biol Chem* 277:3878–3885, 2002

48. Murphy EJ, Prows DR, Stiles T, Schroeder F: Liver and intestinal fatty acid-binding protein expression increases phospholipid content and alters phospholipid fatty acid composition in L-cell fibroblasts. *Lipids* 35:729–738, 2000

49. Kolesnick RN: 1,2-Diacylglycerols but not phorbol esters stimulate sphingomyelin hydrolysis in GH3 pituitary cells. *J Biol Chem* 262:16759–16762, 1987